Extended Abstracts of the 2016 International Conference on Solid State Devices and Materials, Tsukuba, 2016, pp509-510

K-6-04

Diffused Back Surface Field Formation in Combination with Two-Step H_2 Annealing for Improvement of SiNW-Based Solar Cell Efficiency

Wipakorn Jevasuwan, Chen Junyi, Thiyagu Subramani,
Kiyomi Nakajima, Yoshimasa Sugimoto and Naoki Fukata

International Center for Materials Nanoarchitectonics,
National Institute for Materials Science,
1-1 Namiki, Tsukuba, Ibaraki 305-0044, Japan

Abstract

Silicon nanowire (SiNW)-based solar cell fabrication was developed using combination of diffused back surface field formation and two-step H_2 annealing for efficiency enhancement. Two different n-SiNW structures synthesized by metal-catalyzed electroless etching and nanoimprinting followed by Bosch process were applied. The efficiencies for a 1-cm^2 active area of the single-junction SiNW solar cells were achieved upon 7%. Improvement of carried extraction through built-in electric field together with reduction of defect densities on n-SiNW surface and inside p-Si layer could be accomplished.

1. Introduction

Nanowires (NWs) have attracted a great deal of research interest for next-generation solar cells because of many advantages of their structures compared to planar [1]. Metal-catalyzed electroless etching (MCEE), chemical vapor deposition (CVD), and nanoimprinting followed by Bosch process [2-4] are promising to form NW structures on low cost substrates and to apply for a large scale fabrication. However, to realize the device targets, all appropriate fabrication processes of SiNW-based solar cell are important issues to provide good synthesized materials and junction properties through entire solar cell structures. From our previous study [5], SiNW surface passivation and the improvement of SiNW-based solar cell efficiencies using two-step H_2 annealing have been reported. Single-junction solar cells consisting of n-SiNWs and CVD grown p-Si matrix were demonstrated. Two-step H_2 annealing at 900 ˚C for 10 min after both n-SiNW formations and subsequent p-Si matrix deposition effectively improved SiNW surface and p-Si crystallinity, resulting in higher solar cell efficiency.

In this study, back surface field (BSF) or n$^+$ layer formation was further introduced into solar cell fabrication processes. With BSF layer, better electron transportation and reflection of hole by the built-in electric field of n-n$^+$ junction suggest the increasing of the short-circuit current (I_{sc}) [6]. This abrupt junction also induces the increasing of open-circuit voltage (V_{oc}). Therefore, adding of BSF layer into SiNW-based solar cell structure is mandatory. Spin coating of phosphorus containing solution with annealing technique was selected to apply for good compatibility with two-step H_2 annealing and unchanging of solar cell thickness. Both of simple BSF coating with N_2 annealing and modification of annealing process were investigated. Reduction of the second H_2 annealing after CVD and N_2 annealing after BSF coating to only once of H_2 annealing after BSF coating was examined. Various times of this H_2 annealing was also optimized.

2. Experimental Details

Experiments were carried out using n-type Si(100) and Si(111) wafers with a resistivity of 30-50 Ω·cm and thickness of 525 µm as substrates. n-SiNW structures were prepared using two different methods of MCEE or nanoimprinting followed by Bosch process. Approximate 1-µm-length SiNWs were defined for both synthesis methods according to our previous optimization of SiNW length using controlled p-Si coverage and B concentration [7]. Then, the first H_2 annealing was performed at 900 ˚C for 10 min. Prior to p-Si deposition, all n-SiNW surfaces were etched in 1.1M HF in 2.6M isopropanol for SiO_2 removal and immediately set into CVD chamber. p-Si matrix formation was conducted at 750 °C with B doping concentration of ~4×10^{19} cm^{-3}. The flow rate of SiH_4, B_2H_6, and N_2 gases were controlled at 19, 0.5, and 30 sccm, respectively, under chamber pressure of 800 Pa. Then, the second H_2 annealing was performed at 900 ˚C for 10 min. Spin coating of phosphorus containing solution (OCD P-59210) on the back side of substrate was executed and followed by N_2 annealing for 20 min [7]. To provide solar cell electrodes, 200-nm-thick Al front electrode with finger-grid pattern

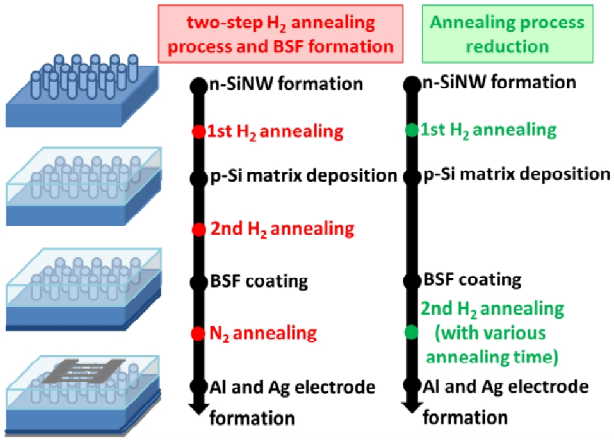

Fig. 1 Schematic of SiNW-based solar cell structure and summarized processes of BSF in combination with two-step H_2 annealing and the reduced annealing process.

and 150-nm Ag back contact were sputtered. Schematic of SiNW-based solar cell structure and the processes of BSF in combination with two-step H_2 annealing and reduced annealing process are summarized in Fig.1. The second H_2 annealing of reduced annealing process was varied to 10, 20 and 30 min.

3. Experimental Results and Discussions

Figure 2 shows J–V characteristics measured under AM1.5G at RT and EQE of (a) MCEE- and (b) nanoimprinting-SiNW solar cells fabricated using two-step H_2 annealing with and without BSF, and reduced annealing process with the second H_2 annealing for 20 min. Obviously, with two-step H_2 annealing, the efficiency (η) of both two structures could be greatly improved, especially at short wavelength range show in EQE spectra. The explanation related to the decreasing of interfacial defect densities on n-SiNW surface and inside p-Si matrix. The V_{oc} and fill factor (FF) were also enhanced by H_2 annealing owing to lower defect densities. With BSF formation, the EQE at long wavelength increased owing to decreasing of surface recombination in bulk Si near the back contact. However, there was a loss at short wavelength range possibly because of exceeding thermal annealing. N_2 annealing of BSF diffusion after the second H_2 annealing might also affect H_2 treatment inside and near the top of p-Si layer.

Hence, the improvement of cell characteristics (J_{sc}, V_{oc}, FF) by BSF formation was not evidently clear due to this material degradation. This issue was well solved by carrying out only the second H_2 annealing after BSF coating to reduce the annealing times. Compared with the previous results, EQE at long wavelength range was slightly lower indicating that P diffusion was not well performed under H_2 ambient. Nevertheless, the degradation of EQE at short wavelength range was minimized resulting in increasing of J_{sc} and V_{oc}. The reduced annealing process could obtain these better solar cell performance agreed with the

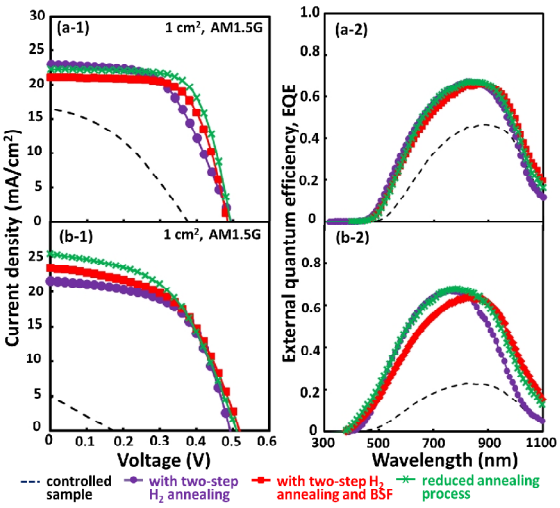

Fig. 2 J–V characteristics measured under AM1.5G at RT and EQE of (a) MCEE- and (b) nanoimprinting-SiNW solar cells fabricated using two-step H_2 annealing with and without BSF, and reduced annealing process with the second H_2 annealing for 20 min.

Table I Summarized solar cell characteristics of all MCEE- and nanoimprinting-SiNW solar cells.

	J_{sc} (mA/cm²)	V_{oc} (V)	FF	η (%)
MCEE-SiNW solar cell	16.53	0.38	0.38	2.4
with two-step H_2 annealing	23.06	0.50	0.55	6.3
with two-step H_2 annealing and BSF	21.07	0.48	0.67	6.8
with reduced annealing process	22.26	0.49	0.68	7.5
Nanoimprinting-SiNW solar cell	12.60	0.16	0.27	0.5
with two-stepH_2 annealing	21.57	0.49	0.58	6.1
with two-step H_2 annealing and BSF	23.37	0.51	0.52	6.3
with reduced annealing process	25.35	0.51	0.53	6.5

dependence of bulk carrier life time on the annealing process [8]. The efficiency upon 7% for a 1-cm^2 active area of the single-junction MCEE-SiNW solar cell was achieved. Solar cell characteristics of all MCEE- and nanoimprinting-SiNW solar cells were summarized in Table I. H_2 annealing time of the reduced annealing process is now in progress to optimize.

4. Conclusions

BSF improved FF of MCEE-SiNW solar cell and J_{sc} and V_{oc} of nanoimprinting-SiNW solar cell, resulting in efficiency enhancement. The reduction of annealing process maintained the H_2 annealing effect for p-Si layer together with improvement of carried extraction by BSF. The results from these fundamental studies encourage the future progress of tandem structures or more advanced designs using new selective substrates for next-generation solar cells.

Acknowledgements

This work was supported in part by the Funding Program for Next Generation World-Leading Researchers (the NEXT Program), JSPS Kakenhi Grant numbers 26600049 and 26246021 and the World Premier International Research Center Initiative (WPI Initiative), MEXT, Japan.

References

[1] B. Tian, X. Zheng, T. J. Kempa, Y. Fang, N. Yu, G. Yu, J. Huang, and C. M. Lieber, Nature **449** (2007) 885.

[2] Y. Hu, K.-Q. Peng, L. Liu, Z. Qiao, X. Huang, F.-Q. Zhang, R.-N. Sun, X.-M. Meng, and S.-T. Lee, Nano Lett. **14** (2014) 4212.

[3] Z.-X. Yang, N. Han, M. Fang, H. Lin, H.-Y. Cheung, S. Yip, E.-J. Wang, T. Hung, C.-Y. Wong, and J. C. Ho, Nat. Commun. **5** (2014) 5249.

[4] Y. Yang, K. Mielczarek, A. Zakhidov, and W. Hu, ACS Appl. Mater. Interfaces **6** (2014) 19282.

[5] W. Jevasuwan, K. Nakajima, Y. Sugimoto, and N. Fukata, Jpn. J. Appl. Phys. **55** (2016) 065001.

[6] S. R. Dhariwal, and A. P. Kulshreshtha, Solid-state Electro. **24** (1981) 1161.

[7] M. Dutta, and N. Fukata, Nano Energy **11** (2015) 219.

[8] K. von Maydell and H. N. Nickel, Appl. Phys. Lett. **90** (2007) 132117.